Electrochemical investigations into ferrocenylphosphonic acid functionalized mesostructured porous nanocrystalline titanium oxide films.

Eugenia Martinez-Ferrero, David Grosso, Cédric Boissière, Clément Sanchez, Olivier Oms, Dominique Leclercq, André Vioux, Fabien Miomandrec, Pierre Audebert

Electrochemical investigations into organized functionalized mesoporous nanocrystalline titanium oxide films.

Eugenia Martinez-Ferrero,[a,#] David Grosso,[a,#] Cédric Boissiere,[a,#] Clément Sanchez,*[a,#] Olivier Oms,[b] Dominique Leclercq,[b] André Vioux,[b,#] Fabien Miomandre[c] and Pierre Audebert*[c]

[a] Laboratoire Chimie de la Matière Condensée UMR CNRS 7574, Université Pierre et Marie Curie-Paris 6, Paris, France

[b]Chimie Moléculaire et Organisation du Solide, UMR CNRS 5637, cc 007, Université Montpellier 2, Place E. Bataillon, F34095 Montpellier cedex 5, France

[c]Laboratoire de Photophysique et Photochimie Supramoléculaires et Macromoléculaires, UMR CNRS 8531, Ecole Normale Supérieure de Cachan, 61 Avenue du Président Wilson 94235 Cachan cedex, France.

Introduction

During the last two decades, the development of organic- inorganic hybrid materials has been associated with the evolution of sol-gel process.[1-3] Furthermore, a wide class of hybrids involves the covalent bonding of the organic and the inorganic components through the use of coupling molecules. Some of us have recently demonstrated the potentialities of phosphonate and phosphinate groups in the coupling of organic components to metal oxides.[4-8] Actually, this coupling is quite stable and difficult to hydrolyze.

Meanwhile the apparition of the first micellar templated materials prepared by sol-gel route has introduced a new type of extremely interesting materials due to their highly organized structure [9-10]. Usually, they present a narrow mesopore size distribution easily tunable between 2 and 30 nm, mesoporous cavities of defined geometry (lamellar, spherical or cylindrical) with various degrees of connectivity and a large porous volume (sometimes higher than $1 cm^3.g^{-1}$). Their preparation by the recently developed Evaporation Induced Self Assembly (EISA) process allowed their rapid and easy shaping as nanometric powders, monoliths, fibers, and thin films of optical quality and controlled thickness.[11-13] Due to their very specific porous network, these new materials are thus highly promising candidates for electrochemical investigations, allowing to establish a relationship between the mesostructure and the electron transfer properties within the structure. Cyclic voltammetry and chronoamperometry in turn are choice methods to investigate the specific features of electron transfer in materials. We have already demonstrated that electrochemistry was a suitable tool for the investigations of the nanostructure of materials prepared by sol-gel chemistry [14-17] and

in particular that the fractal dimension of oxide colloids could be determined by electrochemical investigations.[18]

Ferrocenylphosphonic acid has been shown to be a redox-active pH-responsive molecules for which the variations of the half-wave potential of the acid and their salts results from an electrostatic stabilization and not from the nature of the cations. The electrochemical studies of different metal ferrocenylphosphonates have been reported; particularly the redox half wave potential has been shown to be quite sensitive to the bonding mode to the metal atoms.[19-22]

In this paper we report the anchoring of ferrocenic phosphonic acid onto TiO_2 particles, and we describe the electrochemical behavior of ferrocenylphosphonic acid grafted onto nanocrystalline mesostructured anatase titanium dioxide thin films prepared by EISA process, presenting a specific 2D grid-like pore shape. We show the mode of bonding of the ferrocenylphosphonic acid and how the fine analysis of the electron transfer dynamics is indicative of the anisotropic repartition of the ferrocenyl groups within the film, allowing us to estimate the diffusion coefficient characteristic of the charge transfer with pores. The results shed some light on the efficiency of the charge transfer process between grafted organic components and the mesoporous semiconducting TiO_2 film, which might be important for the improvement of Dye Sensitized Solar Cells (D.S.S.C.) efficiency.

Experimental section

Synthesis

Ferrocenylphosphonic acid was prepared according to the literature procedure.[19]

Anchoring of $FcPO_3H_2$ on TiO_2 particles was performed as reported in the liierature.[5] 1.42g of TiO_2 particles (P25 Degussa) with an average particle size of 21 nm and a specific surface area of 45±5 $m^2 g^{-1}$ were added to 144 mg (0.54 mmol) of ferrocenylphosphonic acid in 50 ml of methanol. The suspension was stirred at room temperature for 24 h and the powder was filtered off and washed successively three fold with 30 ml methanol, and two fold with 30 ml acetone and 30 ml diethyl ether, and dried 12 h under vacuum at room temerature.

The mesoporous TiO_2 films were prepared as previously reported in the literature.[23-25] First we prepared a solution containing $TiCl_4$ as inorganic precursor, a volatile solvent made of ethanol and water, and Pluronic F127 block copolymers ($HO(CH_2CH_2-O)_{106}(CH_2CH(CH_3)-O)_{70}(CH_2 -CH_2-O)_{106}H$) as structuring agents. All reagents were used as provided by Sigma-Aldrich company. The following solution composition was adopted: $TiCl_4$:EtOH:H_2O:F127 with molar ratios of 1:40:10:0.005. This transparent and slightly viscous solution was stirred 15 minutes at room temperature for homogenization. The solution

was then deposited by dip coating at the surface of a SnO_2:F (FTO) substrate at constant speed rate of 2.5 mm.s^{-1} in controlled atmosphere. The liquid layers were evaporated at a fixed Relative Humidity (RH) of 15% then transferred and aged in a sealed environmental chamber with a RH fixed either at 70% for 18 hours. Then, the following thermal treatment was applied: 24 hours at 130°C and 3 hours at 350°C for densification of amorphous TiO_2, 10 minutes flash heating at 500°C and 5 minutes flash heating at 550°C. As reported in literature, flash treatments induced the transformation of amorphous TiO_2 into Anatase TiO_2 nanocrystals of about 7-8 nm.[24,26]

The functionalizations were performed by soaking the nano-crystallized mesoporous films into a $1 \cdot 10^{-4}$ M ethanolic solution of ferrocenylphosphonic acid during 3 h. A continuous stirring was applied to keep the solution homogeneous. The resulting samples were rinsed several times with absolute ethanol and dried in air.

Environmental Ellipsometric Porosimetry

Environmental Ellipsometric Porosimetry (EEP) investigations were performed with a Variable Angle Ellipsometer 2000U from Woolam in the range 400-1000 nm by varying the relative humidity of the atmosphere over the TiO_2 films. The porous volume of TiO_2 films was calculated with the Brugemann Effective Medium Approximation (BEMA) from the optical properties of void and of a TiO_2 reference film prepared without structuring agent with the same thermal history as its mesoporous counterpart. The fractions of porous volume filled with water during the analysis were calculated with BEMA from a mix of the dry mesoporous film and the film completely saturated with water. All the details of experimental setup and data treatments have been previously described.[27]

Electrochemistry

Cyclic voltammetry of modified TiO_2 particles was performed on the powder by means of a Radiometer Analytical PGZ 100 potentiostat in a three-electrode cell. A platinum cavity microelectrode provided by the “réseau micro électrode à cavité” of CNRS (France), was used as working electrode, a platinum wire as auxiliary electrode, and a saturated calomel as reference electrode. The electrolyte was KCl (1M in water) and the scan rate was 100 mV s^{-1}.

The electrochemical response of the functionalized mesoporous TiO_2 films was analyzed using slow and fast scan rate cyclic voltammetry and fast chronoamperometry using an efficient ohmic drop compensation equipped with a home-built potentiostat.[28] The medium used for analysis was acetonitrile (SDS, Spectroscopic Grade), with TBAP (Fluka, puriss.) 0.1 M as the supporting electrolyte. The working electrode was a SnO_2:F (FTO) plate coated with

the TiO_2 film, a part of which was masked so that an area of c.a. 1 cm^2 was in contact with the electrolytic solution. A platinum wire was used as a counter electrode with an Ag|AgCl reference electrode. Solutions were degassed by argon bubbling for 15 minutes prior to each experiment.

Results and discussion

Anchoring of $FcPO_3H_2$ on titania particles.

The possibility of anchoring of ferrocenylphosphonic acid on a titania surface has been checked by reacting the acid with TiO_2 particles (P25 Degussa) in methanol at room temperature. The solution was then filtered off and the powder was thoroughly washed to remove unreacted and physisorbed species and then dried before analysis. Elemental analysis shows 0.66 wt% of P corresponding to 2.8 coupling molecules per nm^2 of TiO_2. The ^{31}P NMR spectrum (fig) shows a rather broad signal at δ = 24.1 ppm, similar in shape to the ones observed for phenylphosphonate/TiO_2 particles.[5] The chemical shift is different from the ones of crystalline $FcPO_3H_2$ which shows two peaks in the solid state at 26.7 and 29.6 ppm. The half wave potential of the ferrocenyl group is + 230 mV/SCE. This value is very closed to those found for $FcPO_3HNa$ ($E_{1/2}$ = + 246 mV/SCE in H_2O), $(FcPO_3H)_2Zn\cdot 2H_2O$ ($E_{1/2}$ = + 235 mV/SCE in H_2O), $(FcPO_3H)_2Cd\cdot 3.5H_2O$ ($E_{1/2}$ = + 238 mV/SCE in H_2O), and $(FcPO_3H)_2Mn\cdot 3H_2O$ ($E_{1/2}$ = + 243 mV/SCE in H_2O), whereas it is far from the half wave potentials of $FcPO_3Na_2$ (86 mV/SCE), $(FcPO_3)_2Cd\cdot 2H_2O$ (132 mV/SCE) and $(FcPO_3)_2Mn\cdot 2H_2O$ (135 mV/SCE).[19,21,22] This suggests that one P-OH group of the ferrocenylphosphonic acid is not bonded to the surface and remains free. The results show that ferrocenylphosphonic acid is strongly bonded to the titanium oxide particles by two oxygen titanium bonds.

Structural analysis of TiO_2 nanocrystallized electrode

Careful studies of the calcination process of mesostructured electrode have shown that aging and crystallization of the amorphous TiO_2 to nanocrystalline anatase involved a simultaneous dramatic reorganization of the mesoporous architecture. As-prepared films exhibit body centered cubic mesostructure (space group Im3m) with organized domains preferentially aligned with their [110] direction normal to the interface,[24,26] as shown in the figure 1A. After consolidation of the inorganic mesostructure at 130 °C for 30 min and removal of the surfactant at 350 °C, the unidirectional shrinkage induced by the drying and thermal treatment applies perpendicularly to the surface and provokes the transformation of the initial mesostructure into a contracted cubic structure having orthorhombic symmetry.

Upon crystallization at 500 °C, this latter structure is turned into a grid-like structure of bidirectional mesoporous parallel network standing perpendicular to the substrate surface percolating from the TiO_2 air interface to TiO_2-FTO electrode (Fig. 1B and C, TiO_2-anatase).[25] The thermal treatment was pushed up to 550°C in order to enlarge connectivities between mesopores.

After impregnation of the calcined film with ferrocenylphosphonic acid, the volumetric analysis of the electrode was performed via spectroscopic ellipsometry. TiO_2 impregnated films were perfectly fitted between 400 nm and 1100 nm with a cauchy single layer model, strongly suggesting that the organic probe was homogeneously dispersed within the porous network. Finally, the measurement of the static water contact angle informs about the wettability of the surface. The measurements have been performed with water drops of 2.5 µL on several samples and the average value was determined. TiO_2 surfaces are hydrophilic allowing the expansion of the water drop and, thus, give low contact angles of 27º. On the contrary, the anchoring of the phosphonic acid on the titania left the hydrophobic terminal ferrocene groups on the surface promoting a contact angle value of 50º after dipping in the ferrocenylphosphonic acid solution and washing. The increase of the contact angle corroborates the presence of hydrophobic molecules onto the surface.

The water adsorption-desorption isotherm obtained by EEP is given in the figure 2. From measurements performed in dry air, we determined the TiO_2 film thickness at 221 nm and the total porous volume of the film is 0.40 $cm^3.cm^{-3}$. As the RH increased, the porous film exhibited a slow uptake of water and a sudden steep adsorption at 70% of RH, characteristic of surfactant templated mesoporous films with a narrow pore size distribution.[26-27,29-32] Upon desorption, a large hysteresis characteristic of pores restrictions appears. The parameters of the porous network, that is, pore large diameter, small diameter and size of restrictions were calculated from the isotherm at 7.6 nm, 2.9 nm and 1.4 nm respectively. From these analyses, one can deduce that the TiO_2 used for electrochemical analysis exhibits a porous network characteristic of the grid-like structure previously reported and made of anisotropic mesoporous cavities connected with each other by four microporous windows, as schemed in the figure 3.

Electrochemistry

The response in cyclic voltammetry of the ferrocene moieties included in the mesoporous titanium dioxide film is represented in Fig.4 at various scan rates. The signal exhibits very well behaved peaks, with a tailing characteristic of a diffusion-limited current. The redox potential of the electroactive moieties is + 270 mV vs. AgCl|Ag. Taking into

account a $\Delta E_{1/2}$ of 50 mV between AgCl and SCE (calomel), this value is the same than the one found for the modified titanium dioxide particles and the same mode of anchoring of the phosphonic acid with one P-OH group of the ferrocenylphosphonic acid not bonded to the surface can be proposed. The low increase in the hydrophobicity of the surface after grafting could be explained by the presence of these remaining hydrophilic groups.

Nevertheless, a very interesting feature is the evolution of the peak currents with the scan rate in log-log scale (fig. 5a). First of all, a linear relationship (slope of $\alpha = 0.65 \pm 0.02$) is obtained on nearly 4 orders of magnitude of scan rate, showing that there is no transition in the mass transfer regime on the explored timescale. In the case of electron hopping between redox sites homogeneously distributed in an isotropic medium, a proportionality of the peak current with the square root of scan rate is expected, since hopping can be assimilated to a diffusion process, as shown by Laviron[33] and Andrieux.[34] This is not the case here, since electron diffusion cannot be assumed to be isotropic, but rather restricted within the "channels" of the mesoporous structure. Further investigation to fully understand this really unusual behavior is currently under progress but requires modelization of the diffusion process in geometry like the one schemed in figure 3.

On the other hand, since it is sometimes uneasy to analyze cyclic voltammograms accurately in terms of rate constants, we turned to chronoamperometry measurements. This technique has the advantage to eliminate the difficulties linked to slow electron exchange rate constants at the electrode (provided that the potential step is chosen far enough from the peak potential). As a consequence, it also enables to have insights into the electron pseudo-diffusion kinetics, as forecast[17] and demonstrated in previous situations.[18] Potential steps at least 200 mV above the ferrocene oxidation potential are applied here, and the current vs time is plotted on a bilogarithmic scale. The results are shown in Fig. 5b. It is clear that a linear relationship is also observed on several orders of magnitude, but with a slope different from the classical value (-0.65 instead of -0.5). Thus, the chronoamperometry measurements confirm the results obtained from cyclic voltammetry as concerns the non-isotropic electron diffusion process in this kind of material. This very unusual behavior has never been observed so far in a modified electrode.

From the current variation with time or scan rate, it is possible to draw an estimation of the apparent diffusion coefficient for electron transfer between ferrocene moieties;[35] in the case of cyclic voltammetry, the Randles-Sevcik relationship can be written: ‡

$$D_{app} = \left(\frac{p}{0.44nFAc_{Fe}} \right)^2 \frac{RT}{nF}$$

$$v_t = \frac{D}{\ell^2} \frac{RT}{nF}$$

where n is the number of electron exchanged per ferrocene unit (n = 1), A is the active area of the electrode, c_{Fe} is the volumic concentration of Fe in the material and p is the slope of the I vs. v relationship (other symbols have their usual meanings). The iron amount can be deduced from integration of the CV curve obtained at very low scan rate (10 $mV.s^{-1}$), assuming that all the ferrocene moieties of the material layer are oxidized at this timescale. A concentration of ca. 8.10^{-5} $mol.cm^{-3}$, corresponding to ca. 0.2 % (in mass) of Fe vs. TiO_2 was found.

From this value of c_{Fe} and taking the geometric area of the electrode (1 cm^2), a diffusion coefficient D_{app} of ca. $4 \cdot 10^{-10}$ $cm^2.s^{-1}$ was obtained from the CV analysis. This value is in good agreement with similar measurements in the case of adsorbed redox molecules in mesoporous films of TiO_2,[36] where the great amount of adsorbed molecules made the diffusion process much more likely to be due to electron hopping than to actual motion of species in solution, thus making the comparison with our results suitable.

In such conditions, the transition between the diffusion limited (at short timescale) and the thin layer (at long timescale) regimes can be estimated to occur for the following scan rate:

where λ is the thickness of the material layer deposited on the electrode (λ = 221 nm). Equation (2) gives v_t = 20 $mV.s^{-1}$, which validates the assumption made for the calculation of c_{Fe}. This means that a thin-layer behavior is likely to be observed at scan rates much lower than this transition value.

Acknowledgements

The authors thank the NOE FAME for financial support and integration activities, and the "réseau microelectrode à cavité" of CNRS France for the gift of a cavity microelectrode. E. M-F thanks the Conselleria d'Empresa, Universitat i Ciència of the Generalitat Valenciana for a postdoctoral fellowship.

Conclusions

We have described the preparation of functionalized mesoporous titanium oxide layers, and the first fast electrochemical study allowing us to have insights on the mode of anchoring of the ferrocenylphosphonic acid and the short range charge transfer features inside the film.

Surprisingly, a very unusual time-current dependence has been observed, which could be indicative of restricted charge pseudo-diffusion within the localized mesopores. Further investigations are in progress to model the electron transfer in such peculiar geometry of modified electrodes. On the other hand, the quality of the charge transfer at the hybrid organic-inorganic interfaces demonstrates that this transfer between the grafted organic component and the mesoporous titania is likely not the limiting step in the preparation of high efficient D.S.S.C.[37]

Notes and references

‡ Despite the non-classical diffusion mode observed here, we use the Randles-Sevcik equation, which should provide an estimation of the order of magnitude of the electronic diffusion coefficient.

1 P. Judeinstein and C. Sanchez, *J. Mater. Chem.,* 1996, **6**, 511.

2 C. Sanchez, H. Arribart, M. M. Giraud-Guille, *Nature Mater.*, 2005**, 4**, 277.

3 A. Clearfield in *Progress in Inorganic Chemistry*, K. D. Karlin (ed.), vol. 47, p 371. New York:Wiley, 1998.

4 G. Guerrero, P. H. Mutin and A. Vioux, *Chem. Mater.*, 2000, **12**, 1268.

5 G. Guerrero; P. H. Mutin and A. Vioux, *Chem. Mater.*, 2001, **13**, 4367.

6 M. Mehring, V. Lafond; P. H. Mutin and A. Vioux, *J. Sol-Gel Sci. Tech.*, 2003, **26**, 99.

7 A. Vioux, J. Le Bideau, P. H. Mutin and D. Leclercq, *Topics Curr. Chem.*, 2004, **232**, 145.

8 G. Guerrero, P. H. Mutin and A. Vioux, *J. Mater.Chem.*, 2005, **15**, 3761.

9 J. S. Beck, J. C. Vartuli, W. J. Roth, M. E. Leonowicz, C. T. Kresge, K. D. Schmitt, C. T-W. Chu, D. H. Olson, E. W. Sheppard, S. B. McCullen, J. B. Higgins and J. L. Schlenker, *J. Am. Chem. Soc.*, 1992, **114**, 10834.

10 S. A. Bagshaw, E. Prouzet and T. J. Pinnavaia, *Science*, 1995, **269**, 1242.

11 C. J. Brinker, Y. Lu, A. Sellinger and H. Fan, *Adv. Mater.*, 1999**, 11**, 579.

12 N. Baccile, D. Grosso and C. Sanchez, *J. Mater. Chem.*, 2003, **13**, 3011.

13 D. Grosso, F. Cagnol G. J. de A. A. Soler-Illia.; E. L. Crepaldi, H. Amenitsch, A. Brunet-Bruneau, A. Bourgeois and C. Sanchez, *Adv. Funct. Mater.* 2004, **14**, 309.

14 P. Audebert, P. Griesmar, P. Hapiot and C. Sanchez, *J. Mater. Chem.*, 1992**, 2**, 12.

15 P. Audebert, C. Demaille and C. Sanchez, *Chem. Mater.*, 1993, **5**, 911.

16 P. Audebert, H. Cattey, C. Sanchez and P. Hapiot, *J. Phys. Chem.*, 1998**, 102**, 1193.

17 P. Audebert, S. Sadki and S. Sallard, *J. Phys. Chem. B,* 2003, **107**, 1321.

18 P. Audebert, S. Sadki, F. Miomandre, G. Lanneau, R. Frantz and J.O. Durand, *J. Mater. Chem.*, 2002, **12**, 1099.

19 O. Oms, F. Maurel, F. Carré, J. Le Bideau, A. Vioux and D. Leclercq, *J. Organomet. Chem.*, 2004, **689**, 2654.

20 O. Oms, J. Le Bideau, F. Leroux, A. van der Lee, D. Leclercq and A. Vioux, *J. Am. Chem. Soc.,* 2004*,* **126***,* 12090.

21 O. Oms, A. van der Lee, J. Le Bideau and D. Leclercq, *Dalton Trans.*, 2005, 1903.

22 O. Oms, J. Le Bideau, A. Vioux and D. Leclercq, *C. R. Chimie*, 2005, **8**, 1237.

23 E. L. Crepaldi, G. J. d. A. A. Soler-Illia, D. Grosso, F. Cagnol, F. Ribot and C. Sanchez, *J. Am. Chem. Soc.*, 2003*,* **125**, 9770.

24 D. Grosso, G. J. d. A. A. Soler-Illia, E. L. Crepaldi, F. Cagnol, C. Sinturel, A. Bourgeois, A. Brunet-Bruneau H. Amenitsch, P. A. Albouy and C. Sanchez, **2003**, *Chem. Mater.*, 2003, **15**, 4562.

25 M. Etienne, D. Grosso C. Boissiere, C. Sanchez and A. Walcarius, *Chem. Commun.,* 2005, **36**, 4566.

26 Y. Sakatani D. Grosso, L. Nicole, C. Boissiere, G. J. de A. A. Soler-Illia and C. Sanchez, *J. Mater. Chem.*, 2006, **16**, 77.

27 C. Boissiere, D. Grosso S. Lepoutre, L. Nicole, A. Brunet-Bruneau and C. Sanchez, *Langmuir*, 2005, **21**, 12362.

28 D. Garreau and J. M. Savéant, *J. Electroanal Chem*, 1975, **50**, 1. 29 A. Brunet-Bruneau, S. Fisson, B. Gallas, G. Vuye and J. Rivory, *Thin Solid Films* 2000*,* **377**, 57.

30 A. Brunet-Bruneau, S. Besson, T. Gacoin, J. P. Boilot and J. Rivory, *Thin Solid Films* 2004, **447**, 51.

31 M. R. Baklanov, K. P. Mogilnikov, V. G. Polovinkin and F. N. Dultsev, **2000**, *J. Vac. Sci. Technol. B,* 2000, **18**, 1385.

32 M. Kuemmel, D. Grosso, C. Boissiere, B. Smarsly, T. Brezesinski, P. A. Albouy, H. Amenitsch and C. Sanchez, *Angew. Chem., Int. Ed.*, 2005, **44**, 4589.

33 E. Laviron, *J. Electroanal. Chem.*, 1980, **112**, 1.

34 C. P. Andrieux and J. M. Savéant, *J. Electroanal. Chem.*, 1980, **111**, 377.

35 A.J. Bard and L.R. Faulkner, *Electrochemical Methods*, chap 6, New York:Wiley, 2000.

36 K.J. McKenzie and F. Marken, *Langmuir*, 2003, **19**, 4327.

37 B. O'Regan and M. Grätzel, *Nature*, 1991, **353**, 737

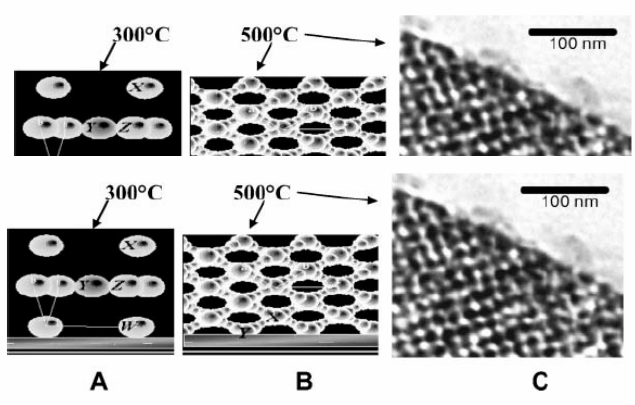

Fig. 1 (adapted from reference 27) Illustration of the mesoporous TiO_2 architecture obtained at (A) 300 °C (closed contracted bcc) and (B) 500 °C (open grid-like). TEM picture of the open grid like structure stabilized at 500 °C (C).

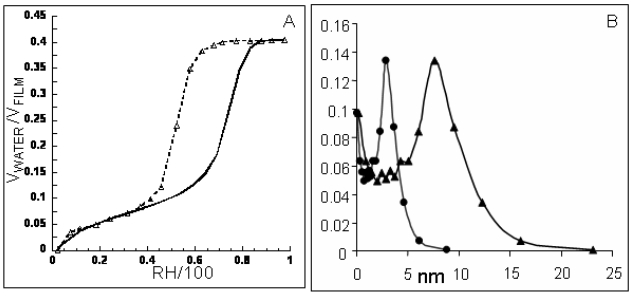

Fig. 2 A) Water adsorption-desorption isotherm obtained from EEP measurements after impregnation of ferrocenylphosphonic acid. B) Pore size distribution of (circles) small axis and (triangles) large axis of ellipsoidal pores obtained from the adsorption branch of the isotherm.

Fig. 3 Nanocrystallized TiO_2 porous network parameters obtained from EEP analysis assuming ellipsoidal pore geometry.

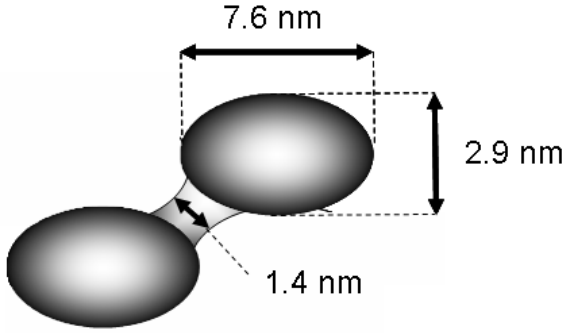

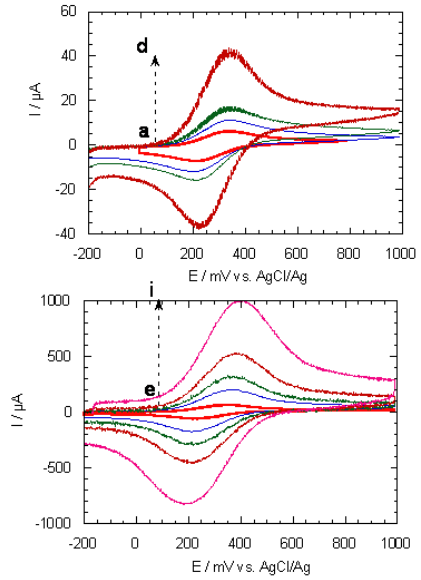

Fig. 4 CVs of the ferrocene grafted mesoporous TiO_2 layer on SnO2:F

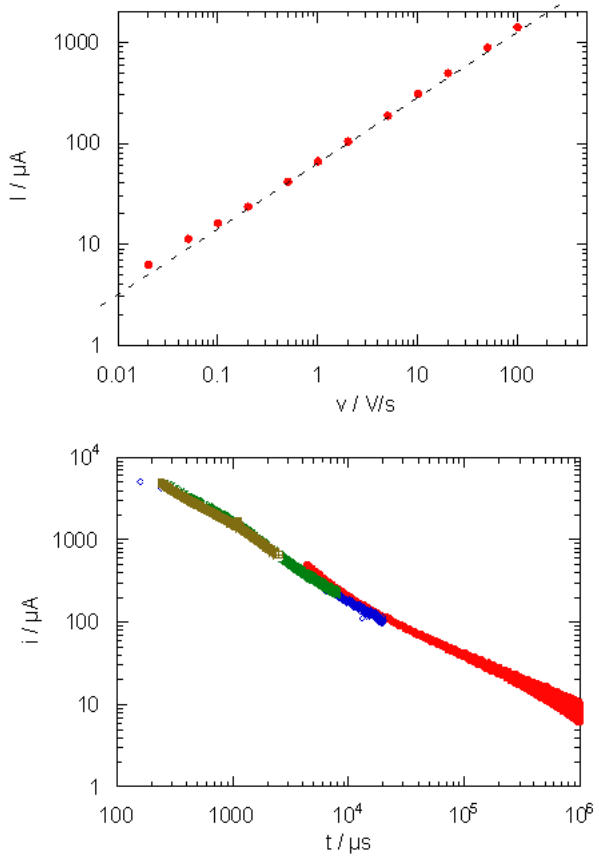

Fig. 5 a) Peak current vs. scan rate in log-log scale for CVs corresponding to figure 4; b) Chronoamperograms in log-log scale of ferrocene grafted mesoporous TiO_2. Applied electrode potential steps from -0.6 to 0.6 V for

various time scales.electrode, at following scan rates (in V/s) : a) 0.02 ; b) 0.05 ; c) 0.1 ; d) 0.5 ; e) 1 ; f) 5; g) 10 ; h) 20 ; i)50.